Raman amplification and lasing in SiGe waveguides

**Ricardo Claps, Varun Raghunathan, Ozdal Boyraz, Prakash Koonath,
Dimitrios Dimitropoulos and Bahram Jalali**

*Optoelectronic Circuits and Systems Laboratory,
University of California, Los Angeles
Los Angeles, CA 90095 USA
jalali@ucla.edu*

http://www.ee.ucla.edu/labs/oecs/

Abstract: We describe the first observation of spontaneous Raman emission, stimulated amplification, and lasing in a SiGe waveguide. A pulsed optical gain of 16dB and a lasing threshold of 25 W peak pulse power (20 mW average) is observed for a $Si_{1-x}Ge_x$ waveguide with x=7.5%. At the same time, a 40 GHz frequency downshift is observed in the Raman spectrum compared to that of a silicon waveguide. The spectral shift can be attributed to the combination of composition- and strain-induced shift in the optical phonon frequency. The prospect of Germanium-Silicon-on-Oxide as a flexible Raman medium is discussed.

©2005 Optical Society of America

OCIS codes: (230.7370) Waveguides; (250.3140) Integrated optoelectronic circuits; (250.4480) Optical amplifiers; (290.5860) Raman Scattering; (040.6040) Silicon

References and links

1. R. Claps, D. Dimitropoulos, Y. Han, B. Jalali, "Observation of Raman emission in silicon waveguides at 1.54 µm," Opt. Express **10**, 1305-1313 (2002).
http://www.opticsexpress.org/abstract.cfm?URI=OPEX-10-22-1305
2. R. Claps, D. Dimitropoulos, V. Raghunathan, Y. Han, and B. Jalali, "Observation of stimulated Raman amplification in silicon waveguides," Opt. Express **11**, 1731-1739 (2003),
http://www.opticsexpress.org/abstract.cfm?URI=OPEX-11-15-1731
3. Liang TK, Tsang HK; "Efficient Raman amplification in silicon-on-insulator waveguides," Appl. Phys. Lett. **85**, 3343-3345 (2004).
4. O. Boyraz and B. Jalali, "Demonstration of a silicon Raman laser," Opt. Express **12**, 5269-5273 (2004),
http://www.opticsexpress.org/abstract.cfm?URI=OPEX-12-21-5269
5. H. Rong, A. Liu, R. Jones, O. Cohen, D. Hak, R. Nicolaescu, A. Fang, M. Paniccia, "A continuous-wave Raman Silicon Laser," Nature **433**, 425-427 (2005).
6. R. Claps, V. Raghunathan, D. Dimitropoulos, and B. Jalali, "Anti-Stokes Raman conversion in silicon waveguides," Opt. Express **11**, 2862-2872 (2003),
http://www.opticsexpress.org/abstract.cfm?URI=OPEX-11-22-2862
7. V. Raghunathan, R. Claps, D. Dimitropoulos, B. Jalali, "Wavelength conversion in Silicon using Raman induced four-wave mixing," Appl. Phys. Lett. **85**, 34-36 (2004).
8. R. L. Espinola, J. I. Dadap, R. M. Osgood, Jr., S. J. McNab, and Y. A. Vlasov, "Raman amplification in ultra small silicon-on-insulator wire waveguides," Opt. Express **12**, 3713-3718 (2004),
http://www.opticsexpress.org/abstract.cfm?URI=OPEX-12-16-3713
9. Q. Xu, V. R. Almeida, and M. Lipson, "Time-resolved study of Raman gain in highly confined silicon-on-insulator waveguides," Opt. Express **12**, 4437-4442 (2004),
http://www.opticsexpress.org/abstract.cfm?URI=OPEX-12-19-4437
10. V. Raghunathan, O. Boyraz, B. Jalali, "20 dB on-off Raman amplification in Silicon waveguides," Proceedings of CLEO, Baltimore (2005).
11. Rong HS, Liu AS, Nicolaescu R, Paniccia M, Cohen O, Hak D; "Raman gain and nonlinear optical absorption measurements in a low-loss silicon waveguide," Appl. Phys. Lett. **85**, 2196-2198 (2004).

#6711 - $15.00 US
(C) 2005 OSA

Received 28 February 2005; revised 17 March 2005; accepted 19 March 2005
4 April 2005 / Vol. 13, No. 7 / OPTICS EXPRESS 2459

12. M. Paniccia, H.S. Rong, A.S. Liu, "Net continuous wave optical gain in a low loss silicon-on-insulator waveguide by stimulated Raman scattering," Opt. Express **13**, 519-525 (2005), http://www.opticsexpress.org/abstract.cfm?URI=OPEX-13-2-519

13. M.W.C. Dharma-wardana, G.C. Aers, D. J. Lockwood and J.M. Baribeau, "Interpretation of Raman Spectra of Ge/Si ultrathin superlattices," Phys. Rev B **41,** 5319 (1990).

14. M. Robillard, P.E. Jessop, D.M. Bruce, S. Janz, R.L. Williams, S. Mailhot, H. Lafontaine, S.J. Kovacic, J.J. Ojha; "Strain-induced birefringence in Si1-xGex optical waveguides," J. Vac. Sci. Technol. B **16,** 1773-1776 (1998).

15. D.-X Xu, P. Cheben, D. Dalacu, A. Delage, S. Janz, B. Lamontagne, M.-J. Picard, W.N. Ye, "Eliminating the birefringence in silicon-on-insulator ridge waveguides by use of ridge cladding stress," Opt. Lett. **29,** 2384-2386 (2004).

16. R. People, J.C. Bean; "Calculation of critical layer thickness versus lattice mismatch for GexSi1-x/Si strained-layer heterostructures," Appl. Phys. Lett. **47,** 322-324 (1985).

17. G.P. Agrawal, "Nonlinear fiber optics," Academic Press (1995)

18. M.I. Alonso, K. Winer; "Raman spectra of c-Si1-xGex alloys," Phys. Rev. B **39,** 10056-10062 (1989).

19. K. Kutsukake, N. Usami, T. Ujihara, K. Fujiwara, G. Sazaki, K. Nakajima; "On the origin of strain fluctuation in strained-Si grown on SiGe-on-insulator and SiGe virtual substrates," Appl. Phys. Lett. **85,** 1335-1337 (2004).

20. W. Byra, "Raman Scattering in Ge-Si alloys," Solid State Comm. 12, **253** (1973).

21. J.C. Tsang, P.M. Mooney, F. Dacol, J.O. Chou, "Measurements of alloy composition and strain in thin Ge_xSi_{1-x} layers," J. of Appl. Phys. **75,** 8098-8108 (1994).

22. R. A. Logan, J.M. Rowell, and F.A. Trumbore; "Phonon Spectra of Ge-Si Alloys," Phys. Rev. **136,** A 1751-A 1755 (1964).

23. H.K. Shin, D.J. Lockwood, J.-M Baribeau; "Strain in coherent-wave SiGe/Si superlattices," Solid State Comm. **114,** 505-510 (2000).

24. F. Schaffler, "Properties of Advanced Semiconductor Materials GaN, AlN, InN, BN, SiC, SiGe," pp. 149-188, Eds. Levinshtein M.E., Rumyantsev S.L., Shur M.S., John Wiley & Sons, Inc., New York (2001).

25. F. Cerdeira, C.J. Buchenauer, F. H. Pollack and M. Cardona; "Stress-Induced Shifts of First-Order Raman Frequencies of Diamond- and Zinc-Blende-Type Semiconductors," Phys. Rev. B **5,** 580-593 (1972).

26. E. Anastassakis, A. Pinczuk, E. Burstein, F.H. Pollack, M. Cardona; "Effect of static uniaxial stress on the Raman spectrum of silicon," Sol. State Comm. **8,** 133-138 (1970).

1. Introduction and motivation

In the past three years, nonlinear Raman processes in waveguides fabricated on a silicon-on-insulator (SOI) platform has received significant attention [1-12]. This approach has achieved great success, with the recent reports of up to 20 dB of Raman gain in pulsed-pumping mode [10], a 3 dB gain in cw pumping mode [12], and pulsed [4] and cw lasing [5]. In addition, wavelength conversion between the technologically important bands of 1300nm and 1550nm has been demonstrated using the Coherent Anti Stokes Raman Scattering (CARS) phenomenon [6, 7]. However, spectral limitations of the Raman Effect in silicon are unavoidable in the SOI platform. In the case of Raman amplification, the limited bandwidth of the spontaneous Raman signal from silicon (105 GHz) makes it unsuitable for its use in broad-band WDM applications, unless multi-pump schemes are implemented. Also, the large wavelength shift between the pump and the Stokes fields renders phase matching difficult to achieve, hence resulting in low wavelength conversion efficiency for the CARS process.

The introduction of germanium in the overall scheme of nonlinear Raman processes in silicon offers new avenues for tailoring the device characteristics. In particular:

(i) The strain caused by the difference in the lattice constants of Si and Ge along with the composition effect, provide mechanisms for tuning the Stokes shift associated with the dominant Si-Si (500 cm^{-1}) vibrational mode [13]. In addition, the presence of Si-Ge modes (400 cm^{-1}) and Ge-Ge modes (300 cm^{-1}) provide flexibility in pump and signal wavelengths.

(ii) Spectral broadening can be achieved by via graded Ge composition.

(iii) The strain resulting in birefringence [14,15] can provide an addition degree of freedom for phase matching in the wavelength conversion process. Stress also

results in broadening of the gain spectrum, via splitting of the degenerate optical phonon modes.

(iv) When grown on an SOI substrate, the use of double cladding in the vertical direction can improve fiber-waveguide coupling efficiency.

(v) Higher carrier mobility, and hence diffusion constant, in SiGe reduces the effective lifetime in the waveguide. This reduces the losses associated with the free carriers that are generated by Two Photon Absorption (TPA). However, this benefit will be countered by the higher TPA coefficient in GeSi.

2. Waveguide design and fabrication

The platform used to perform the experiments reported here is a Silicon-Germanium-on-Insulator (SGOI) structure with a 1.0 µm buried oxide, a 2.0 µm Si film, a 0.7 µm layer of $Si_{.92}Ge_{.08}$ alloy, and a 0.4 µm Si cap layer. The structure was prepared by Chemical Vapor Deposition (CVD) under nonequilibrium growth condition [16]. The SiGe layer was characterized by Secondary Ion Mass Spectrometry (SIMS) analysis, which indicated a Ge content of 7.5% ±0.5. The waveguide formed via photolithography and Deep Reactive Ion Etching (DRIE). The rib width was 4 µm and the etch depth was 1.4 µm. The modal area of the waveguide was calculated to be $A_{eff} = 5.5$ µm^2 using the Beam Propagation Method. The propagation losses are estimated to be 1dB/cm.

3. Experimental results

The spontaneous Raman signal measured from the SGOI waveguide is shown in Fig. 1. The pump is a CW cascaded cavity fiber Raman laser with a linewidth of ~ 1nm. The measured Stokes Raman peak is overlaid with the Raman signal from an SOI waveguide for comparison and clearly shows a down-shift effect of 45 GHz for the SGOI waveguide. A broadening of approximately 25 GHz at FWHM is also observed.
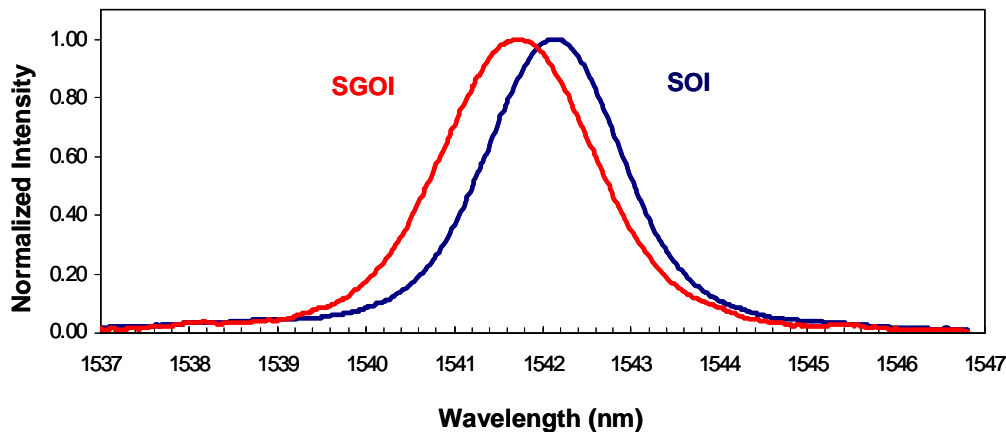

Fig. 1. Spontaneous Raman spectrum from a SiGe waveguide, compared to that of a Silicon waveguide.

A series of pulsed-pump measurements of stimulated Raman amplification were performed using the experimental setup outlined elsewhere [4,10]. Pulsed pumping is employed because of high peak powers that can be attained and to minimize the accumulation of TPA generated free carriers [3]. The pump pulses had 30ps width with 25MHz repetition rate and were centered at 1539nm. The signal laser was CW and was centered at 1673nm. Figure 2 shows the change in the signal power caused by the Raman interaction with the pump. The peak gain

of 16dB is obtained at the average pump power of 46mW. Figure 3 shows a plot of the measured gain as a function of the peak pump pulse power.
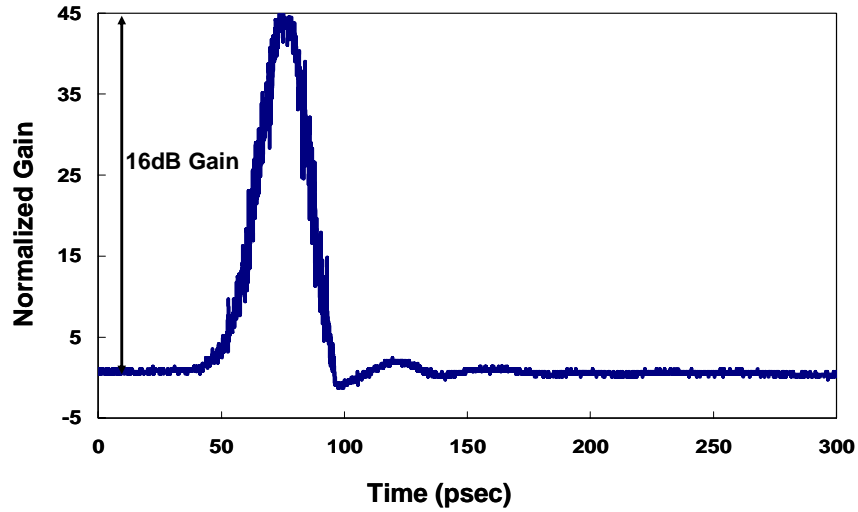

Fig. 2. Time domain trace of the maximum Raman amplification obtained with the SiGe alloy waveguide, using a pulsed pump scheme.
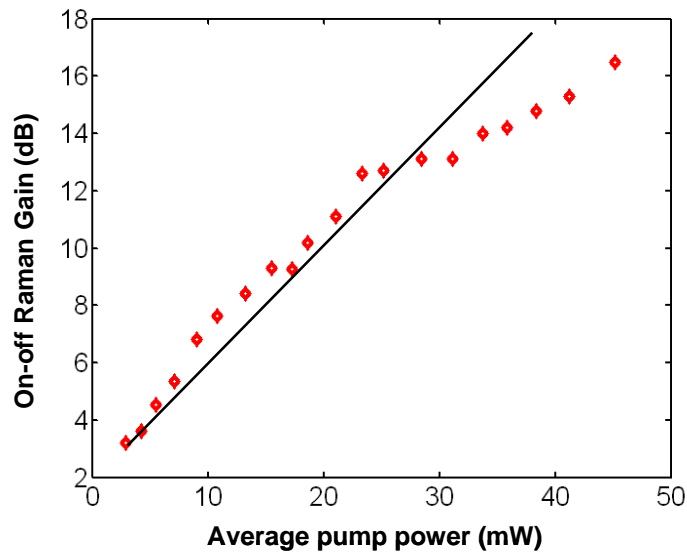

Fig. 3. Gain curve as a function of average pump power in the pulsed pump experiment.

The spectrum for Stimulated Raman Scattering (SRS) was measured by tuning the signal wavelength in the presence of a fixed pump wavelength (1539 nm). The temperature-tuned signal source was a DFB laser with a linewidth of ~ 10MHz. Figure 4 shows the results for the SGOI waveguide compared to that from an SOI waveguide. The data indicates a Stokes down shift of 37GHz, in good agreement with that observed in the spontaneous data of Fig. 1.
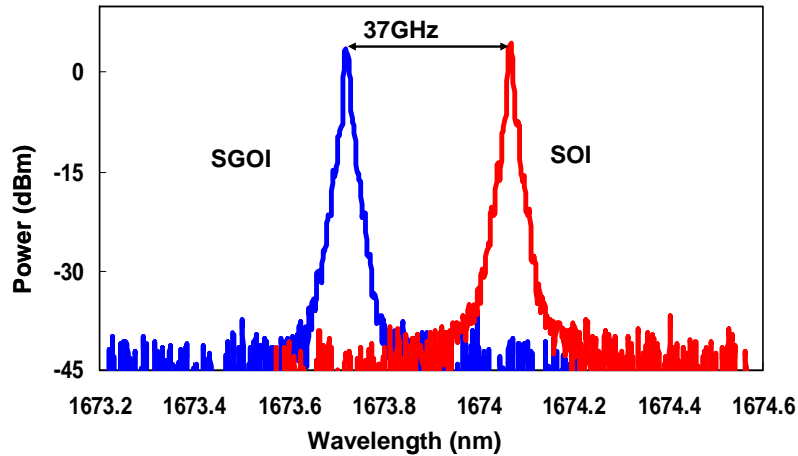
Fig. 4. The signal laser line for the wavelength at which maximum Raman amplification is observed. Two cases are shown: a pure SOI waveguide, and an SGOI waveguide.

Figure 5 shows the measurement of the free carrier lifetime, obtained by de-tuning the cw signal laser off the Raman resonance. This measurement reveals the effects of TPA and free carrier absorption. The transient response consists of fast transient caused by TPA and a slow recovery due to free carrier recombination with an extracted free carrier lifetime of, $\tau = 9$ ns.
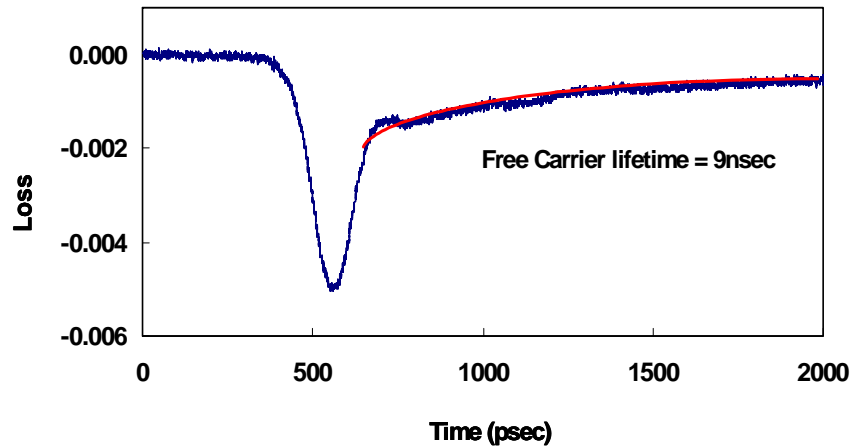

Fig. 5. Free-Carrier lifetime measurements. The cw signal laser has been de-tuned from the Raman resonance of the pulsed pump laser, and a net TPA loss is observed. The slow decay of the FCA effect is clear, and has been fitted to an exponential decay with a lifetime of τ=9 ns.

The above described results for pulsed Raman amplification show that the net gain after the loss in the system (including the coupling losses) was ~5dB. With the objective of creating a lasing device, a cavity was built across the waveguide using a fiber loop, as described elsewhere [4]. The length of the fiber (~8m) was chosen to match the repetition rate of the pump laser. Figure 6 shows the output Stokes power (average) of the Raman laser obtained using a 2% tap coupler from the laser cavity, as a function of the input pump power (average). A linear fit to the data is also shown. The laser threshold is measured to be 20mW average pump power (25W peak power).The saturation of the Stokes emission is due to the EDFA

nonlinearities which broadened the pump spectrum. The pump spectrum begins to broaden in the fiber patchcords and EDFA at about 35 mW average power (45 W peak pulse power). Because of the narrow gain spectrum of Raman in silicon (~ 100GHz) this results in a lowering of the Raman gain coefficient [4].
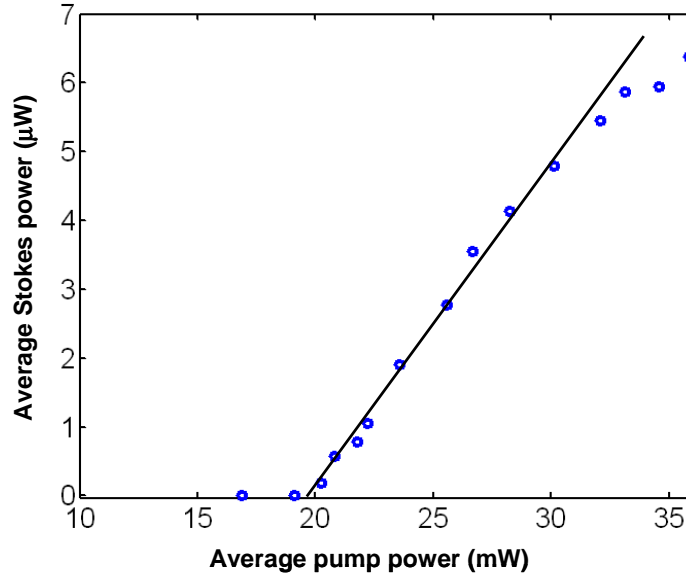

Fig. 6. Variation of the average output Stokes power versus input pump power, for the SiGe laser.

The possibility that the observed lasing is caused by stimulated Raman amplification in the fiber loop can be readily rejected based on the negligible gain in the short length of fiber. Based on the known Raman gain spectrum of fiber [17] the optical gain in the fiber loop is $0.3x10^{-13}$ m/W corresponding to a total gain of 0.35 dB at the threshold pump power. This is negligible compared to the measured round trip loss of 13dB, and hence cannot account for the observed lasing characteristics.

4. Discussions

Figure 7 shows the critical layer thickness for SiGe alloy as a function of the Ge concentration [16]. This limit applies to layers prepared under nonequilibrium growth condition [16] which was the case for our devices. For the structure with 7.5% Ge as used in our experiments, the maximum thickness of a layer that can be grown, defect free, is approximately 1000nm. The 740nm thick film in the waveguide is below this limit and hence is coherently strained. For strained semiconductor alloys, there are two contributions to the Raman Stokes shift, namely the strain effect, and the composition effect. The compositional shift has been attributed to increase in the average mass of Si due to surrounding Ge atoms, resulting in the lowering of the silicon optical phonon frequency [18-21]. The strain effect is caused by the change in the restoring force caused by the change in steady state ion displacement [21-23].
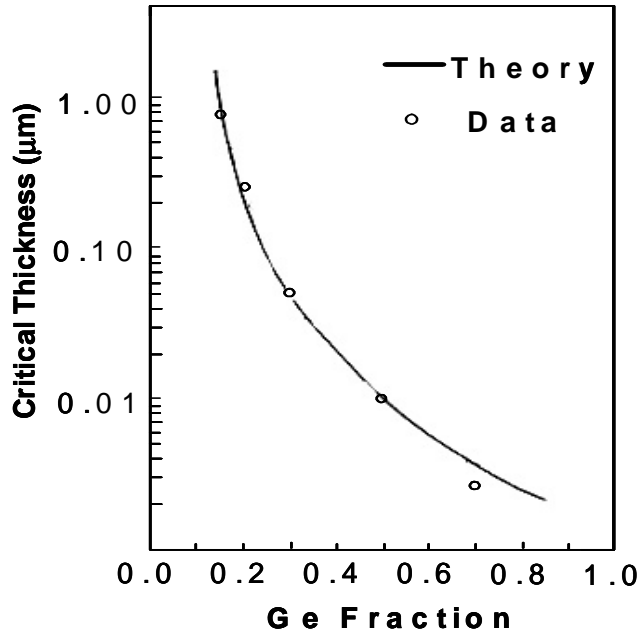
Fig. 7. Critical layer thickness for SiGe alloy as a function of the Ge concentration. After [16].

Down shift of the Raman spectrum to a lower wavelength has previously been observed in spontaneous backscattering from SiGe alloys, and has been attributed to the combination of compositional- and strain-induced effects [18-23]. The compositional effect can be modeled as [20, 21],:

$$\omega_{Si}(\text{cm}^{-1}) = 520.1 - 65\,x \qquad (1)$$

Where, x, is the concentration of Ge in the alloy ($Si_{1-x}Ge_x$). Equation (1) renders a value of -4.87cm^{-1} (145 GHz) for the shift of the Si peak in a 7.5%, Ge alloy. The net shift is however lowered by the presence of strain.

The Strain-induced shift of the Raman frequency of the Si-Si mode in the SiGe alloy, which is compressively strained, can be modeled as [21]:

$$\omega_{Si}(\text{cm}^{-1}) = 520.2 + \Delta \cdot \Sigma \qquad (2)$$

Here, Σ refers to the normalized Strain ($\Sigma \approx x$) and the coefficient Δ has an average value of 29cm^{-1} [21]. Based on the alloy composition in our waveguides (x = 7.5%), we calculate a strain induced shift of +2.17cm^{-1}. This suggests a net shift for the Stokes peak of: -4.87cm^{-1} + 2.17cm^{-1} = -2.7cm^{-1}. This is approximately ~50% larger than the measured value of -1.4 cm^{-1}. This difference can be attributed to the fact that not all optical power is confined within the SiGe alloy, as described below.

For a coherently strained $Si_{1-x}Ge_x$ alloy, the refractive index is given by $n = 3.42 + 0.37 \cdot x + 0.22 \cdot x^2$ [24]. Ge profile measured using SIMS technique is shown in Fig. 8. Also shown is the mode profile obtained using the mode matching technique (FIMMWAVE^{TM}). While the mode is centered in the GeSi alloy, the small index contrast between the alloy and the silicon cladding layers, gives rise to a long evanescent tail extending into the lower cladding layer. This accounts for a smaller shift in the measured Raman peak, compared to the situation where the light is entirely confined in the alloy. The combined contributions of the pure silicon and the alloy spectra caused by the distributed mode profiles will also result in broadening of the Raman peak due to the spectral overlap of the Si and SiGe resonances. Another source for broadening could be the splitting of the triply

degenerate TO-LO optical phonon modes. Splitting of the triply degenerate TO-LO optical phonon mode induced by uniaxial stress has been observed in semiconductors with diamond crystal structure [25]. It occurs by the degenerate phonon mode splitting into a singlet, polarized along the direction of crystal growth, and a doublet, formed by the two phonon modes polarized along the plane orthogonal to this direction. The value of the splitting is given by [26],

$$\Omega_s - \Omega_d = \frac{\tau}{2\omega_0}(p-q)(s_{11} - s_{12}).$$ (3)

where p and q are the phonon deformation potentials for silicon: $p/\omega_0^2 = -1.2$, $q/\omega_0^2 = -1.8$ [26], and s_{ij} are the reduced compliance tensor components: $s_{11} = 76.8$, and $s_{12} = -21.4$, in units of 10^{-14} cm^2 /dyne [13, 26]. The strain for a, $x = 7.5\%$, $Si_{1-x}Ge_x$ alloy layer can be assumed to be: $e_1 = e_2 = 0.0416 \times 0.07$, where 1 and 2 denote the two orthogonal directions along the plane of the alloy layer. The compressive stress component in the plane of the alloy is given by [26],

$$\tau = e_1 /(s_{11} + s_{12}) = -0.529 \text{ GPa},$$ (4)

This suggests a splitting between singlet and doublet modes of, Ω_s - $\Omega_d = 0.84$ cm^{-1}~ 25 GHz, which agrees well with the observed broadening of the Raman peak. However, we note that further study on samples with different Ge concentration, alloy thickness, and higher resolution spectrum measurements are required to draw a precise quantitative conclusion about the spectral shift and broadening. In addition, the role of the nonuniformity in the Ge content, as observed in Fig. 8, on the spectrum broadening must also be quantified.
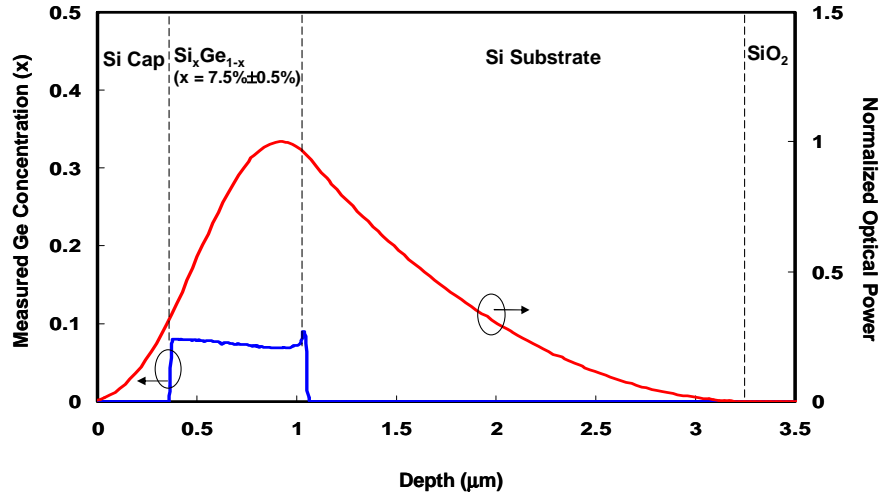

Fig. 8. The spatial profile of the optical mode is shown (red curve) along with the Ge content spatial profile as obtained by a SIMS technique (blue curve)

4. Summary

In summary, we have reported the first observation of spontaneous Raman emission, stimulated amplification, and lasing in a SiGe waveguide. A pulsed optical gain of 16dB and a lasing threshold of 25W peak pulse power is observed for a $Si_{1-x}Ge_x$ waveguide with x=7.5%. At the same time, an approximately 40 GHz frequency downshift is observed in the Raman spectrum compared to that of a silicon waveguide.

Acknowledgments